Supplemental Material

Impact of the synthetic approach on the magnetic properties and homogeniety of mixed crystals of tunable layered ferromagnetic coordination polymers

Carsten Wellm, Anna M. Majcher-Fitas, Michał Rams, and Christian Näther

Content

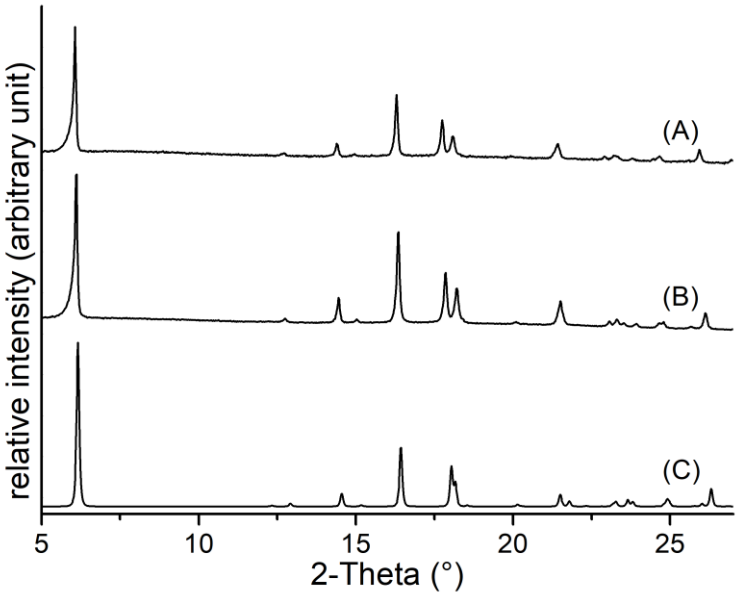

Figure S1. Experimental powder pattern of **2-Ni** (A) and **2-Co** (B) as well as the simulated powder pattern of **2-Ni** (C).

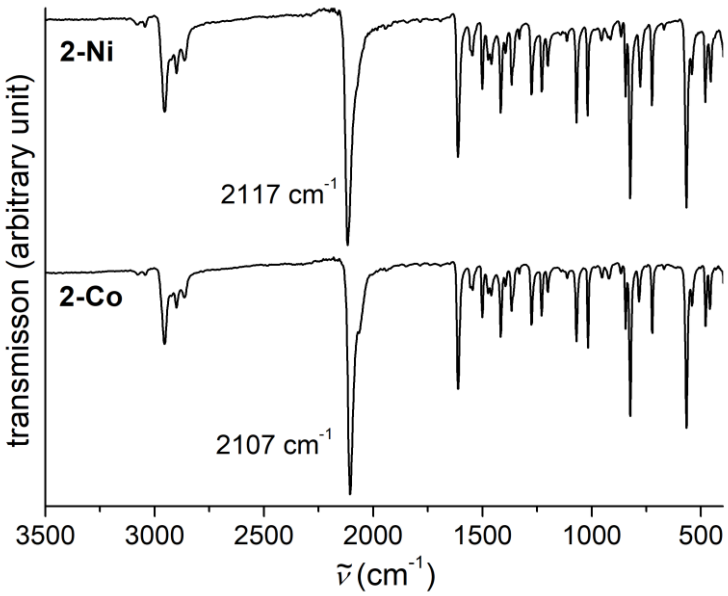

Figure S2. IR-Spectra of **2-Ni** (top) and **2-Co** (bottom). Given are the values of the CN-stretching vibrations.

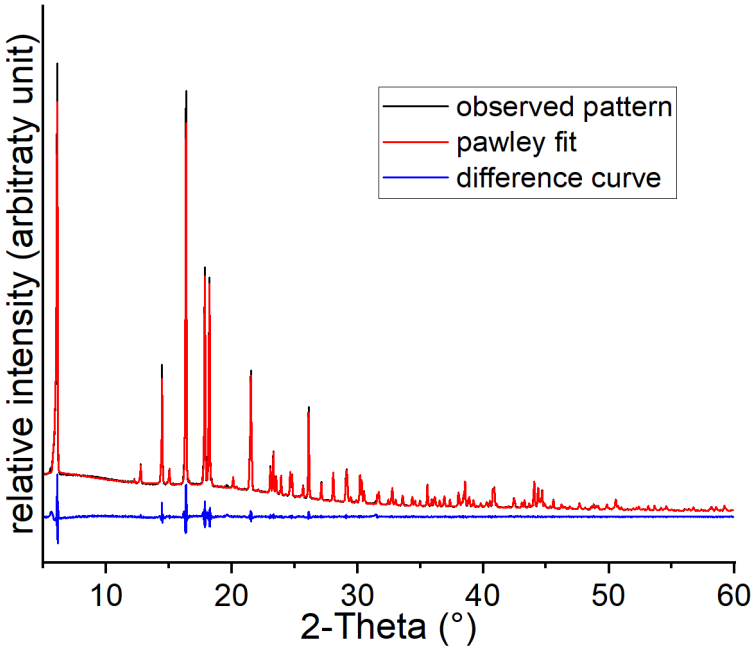

Figure S3. Pawley fit of the powder pattern of **2-Ni**.

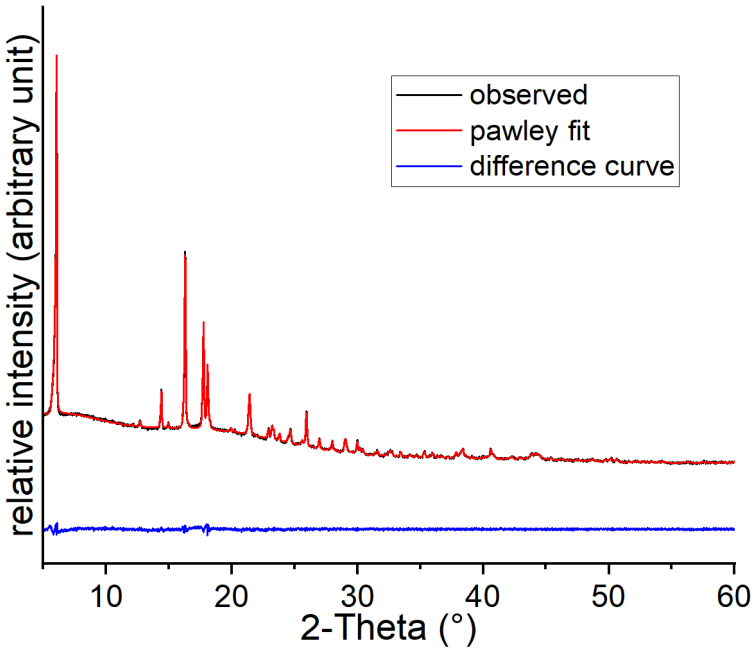

Figure S4. Pawley fit of the powder pattern of **2-Co**.

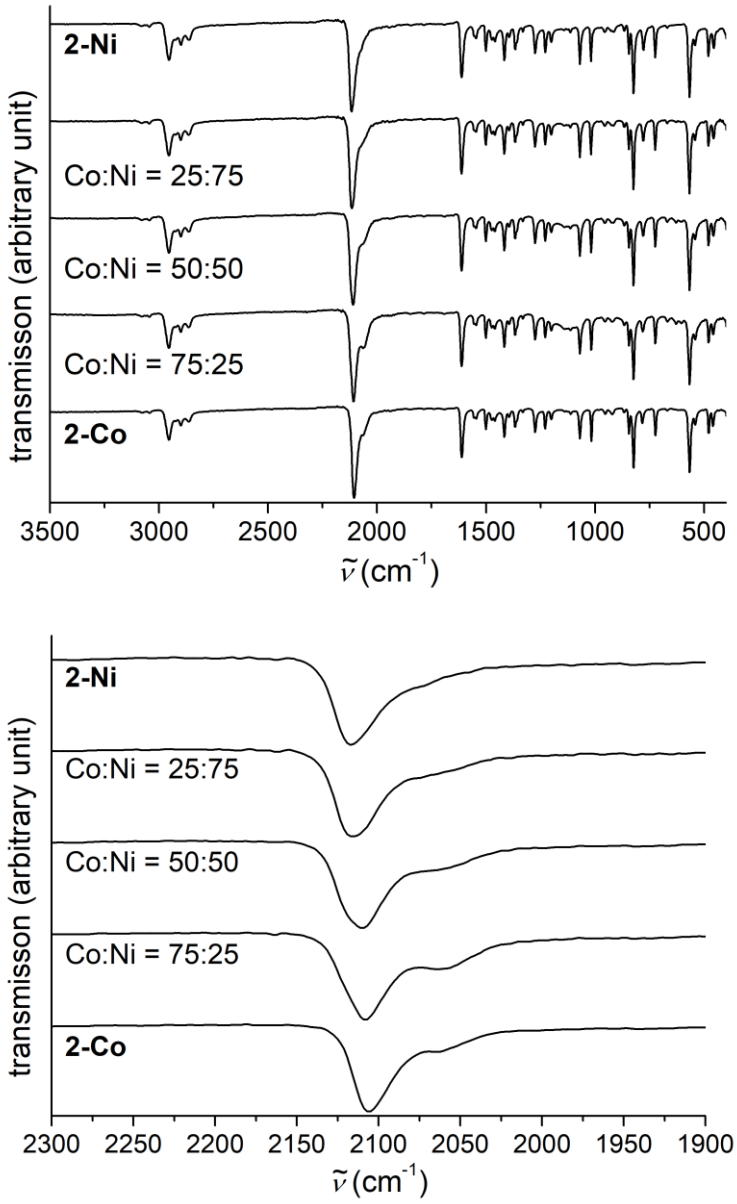

Figure S5. IR spectra of **2-Co**, **2-Ni** and of physical mixtures of **2-Co** and **2-Ni** in different Co:Ni ratios in full range (top) and in the region where the CN stretching vibration is observed (bottom).

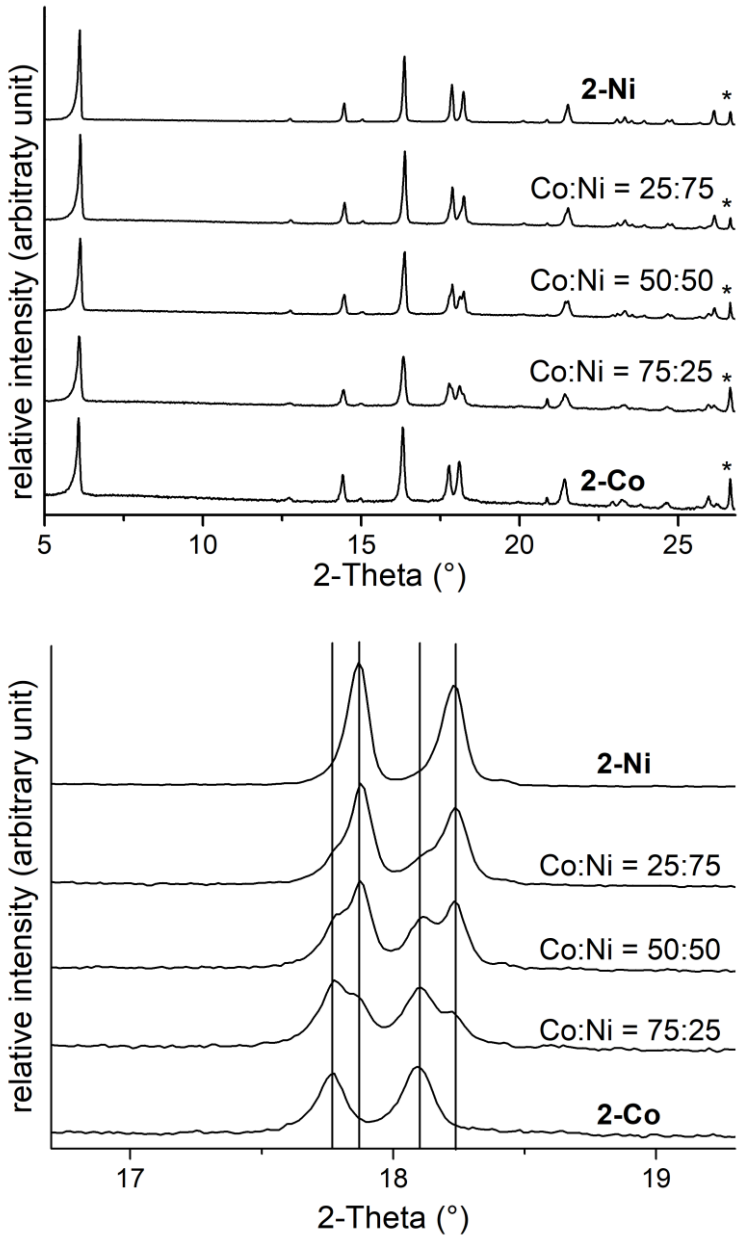

Figure S6. Experimental PXRD pattern of **2-Co**, **2-Ni** and of physical mixtures of **2-Co** and **2-Ni** in different Co:Ni ratios in full range (top) and smaller range (bottom). In the top figure the reflections indicated by an asterisk correspond to α-quartz as internal standard. In the bottom figure the position of the reflection for **2-Ni** and **2-Co** are indicated by solid lines are the (-211) and (-102) reflections.

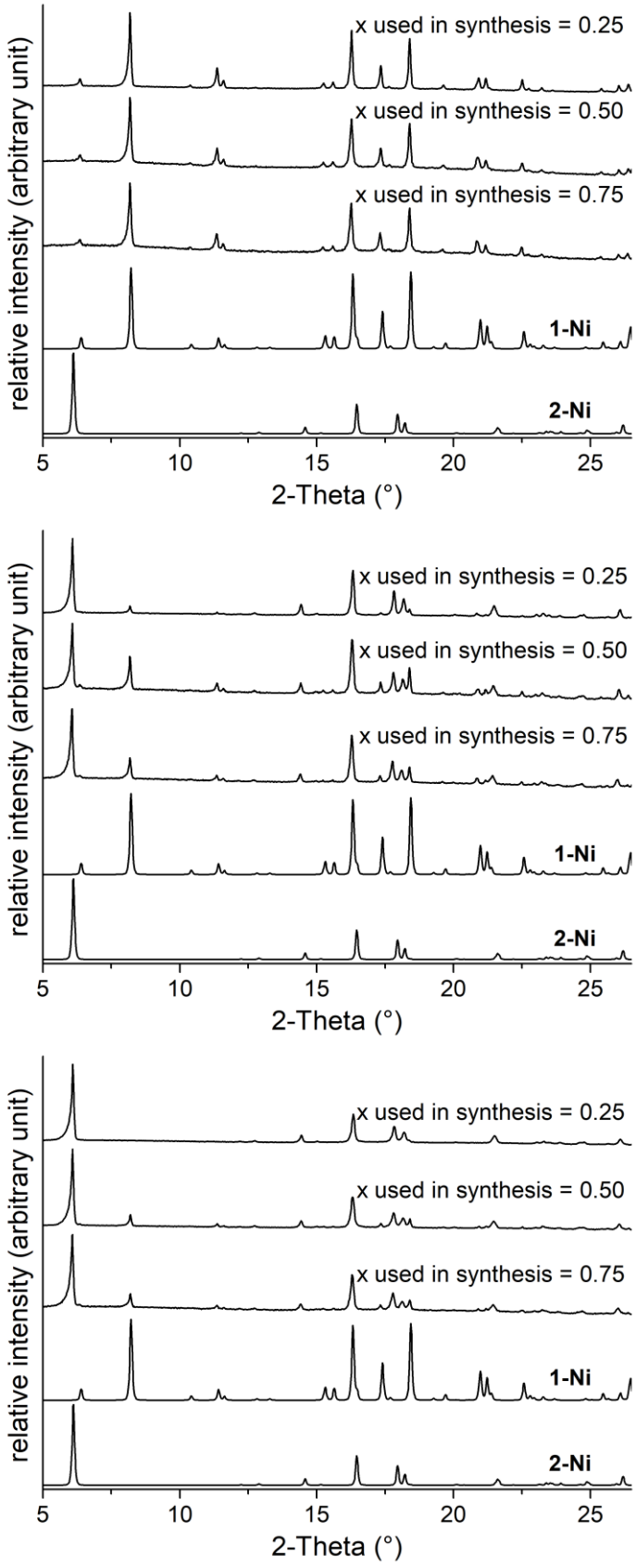

Figure S7. PXRD patterns of the residue of the reaction of x $Co(SCN)_2$ and 1-x $Ni(SCN)_2$ (x = 0.25, 0.5, 0.75) with 4-*tert*-butylpyridine (metal salt to ligand ratio = 1:2) in MeOH (top), EtOH (center) and acetone (bottom), together with the calculated patterns of **1-Ni** and **2-Ni**.

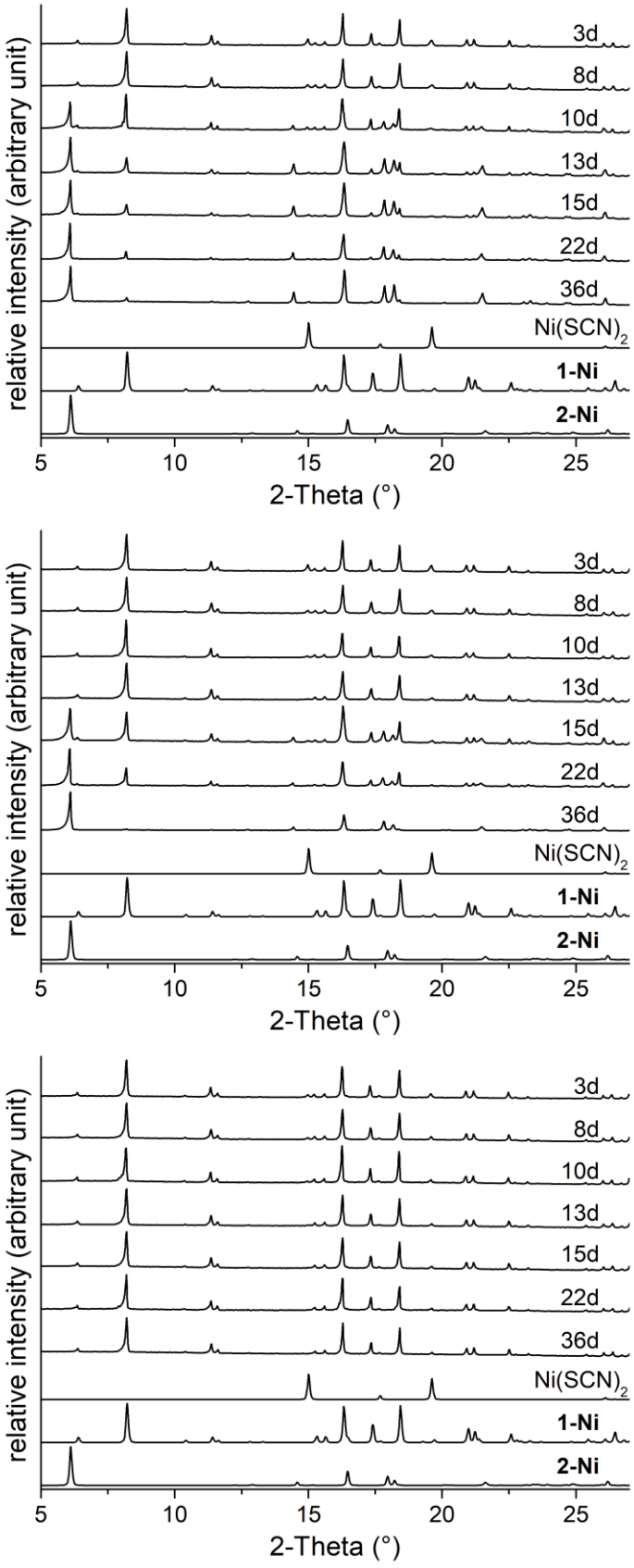

Figure S8. PXRD patterns of the residue obtained at different times during the reaction of x $Co(SCN)_2$ and 1-x $Ni(SCN)_2$ with 4-*tert*-butylpyridine (metal salt to ligand ratio = 1:2) in EtOH for x = 0.25 (top), x = 0.50 center) and x = 0.75 (bottom), together with the calculated patterns of $Ni(SCN)_2$, **1-Ni** and **2-Ni**.

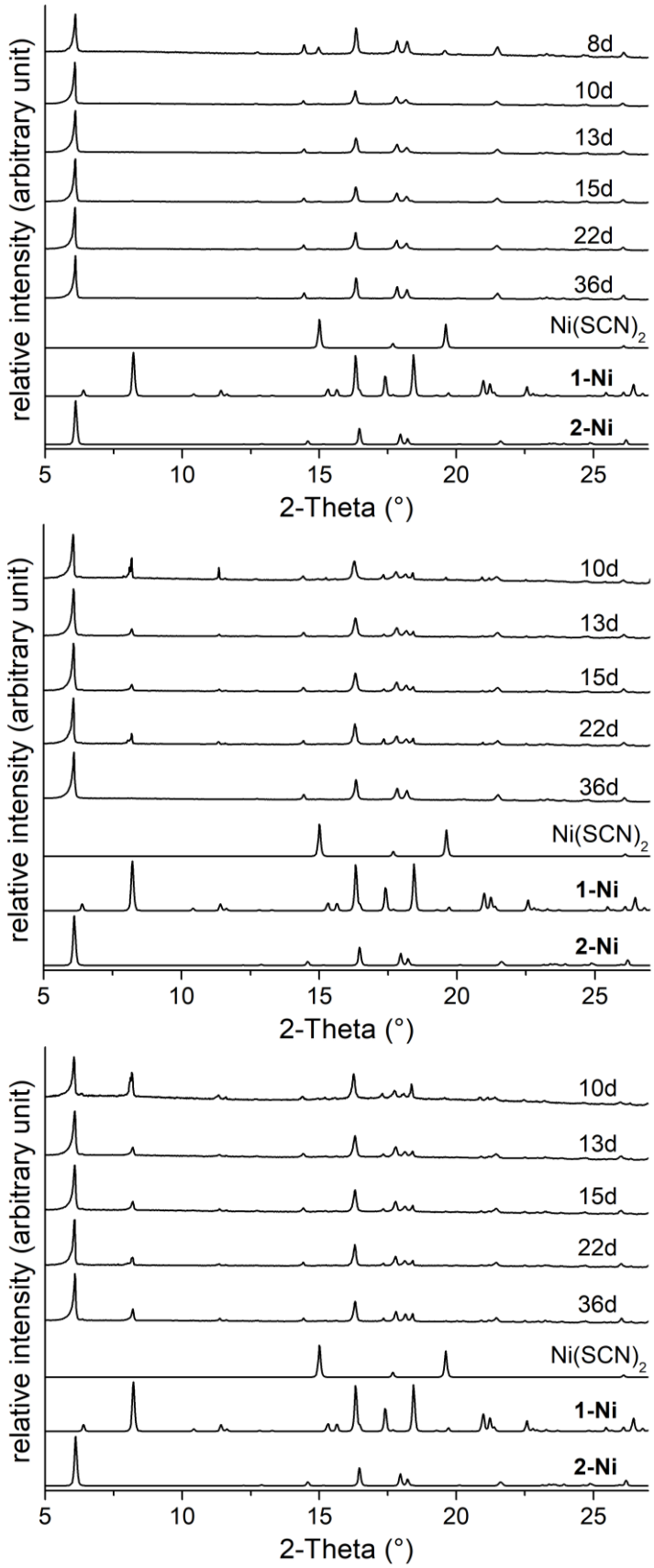

Figure S9. PXRD patterns of the residue obtained at different times during the reaction of x $Co(SCN)_2$ and 1-x $Ni(SCN)_2$ (x = 0.25, 0.50, 0.75) with 4-*tert*-butylpyridine (metal salt to ligand ratio = 1:2) in acetone for x = 0.25 (top), x = 0.50 center), x = 0.75 (bottom), together with the calculated patterns of $Ni(SCN)_2$, **1-Ni** and **2-Ni**.

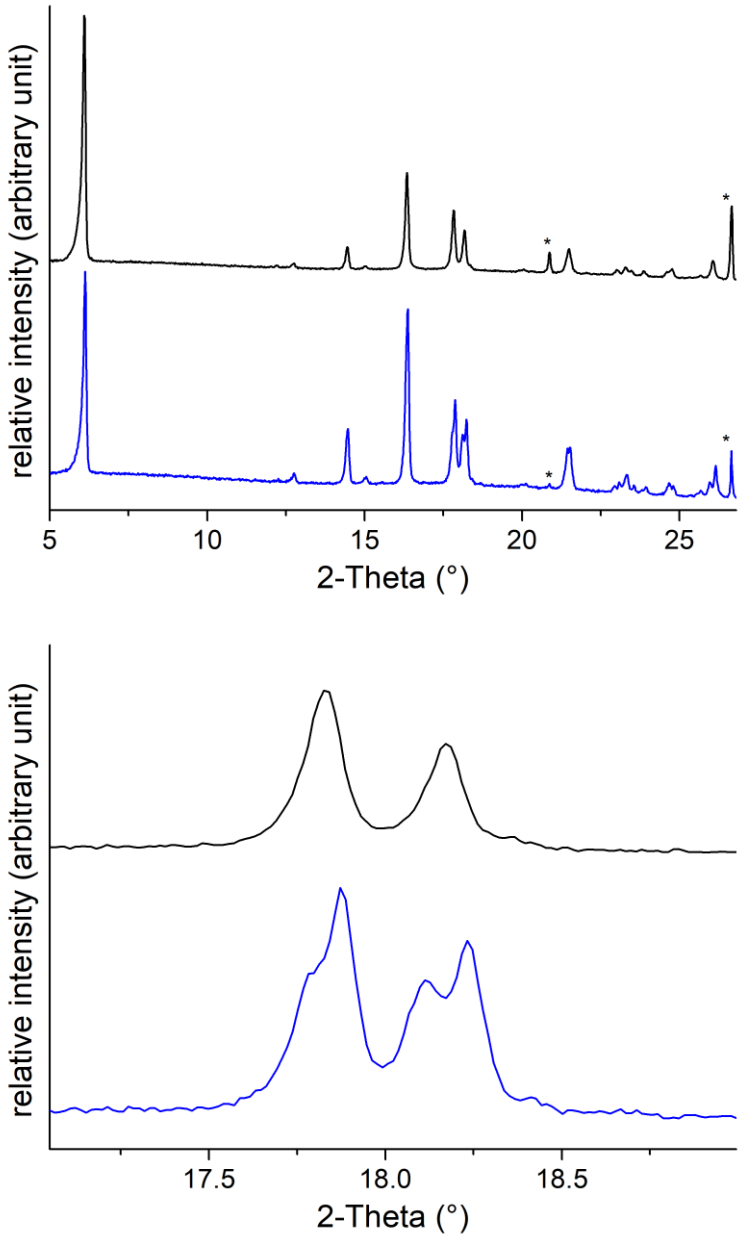

Figure S10. Experimental PXRD patterns of a 1:1 mixture of **2-Co** and **2-Ni** (blue) and the residues obtained after stirring this mixture in ethyl acetate at room temperature for 7 days (black) in full range (top) and a smaller range (bottom). In the top figure the reflections indicated by an asterisk correspond to α-quartz as internal standard.

Table S1. Results of the AAS measurements for samples of mixed crystals of **2-Co_xNi_{1-x}** synthesized at room temperature for 10 d in ethyl acetate.

x **used in synthesis**	**0.25**	**0.50**	**0.75**
Sample 1	0.28	0.50	0.78
Sample 2	0.27	0.50	0.78
Sample 3	0.28	0.51	0.78
Average	**0.28**	**0.50**	**0.78**

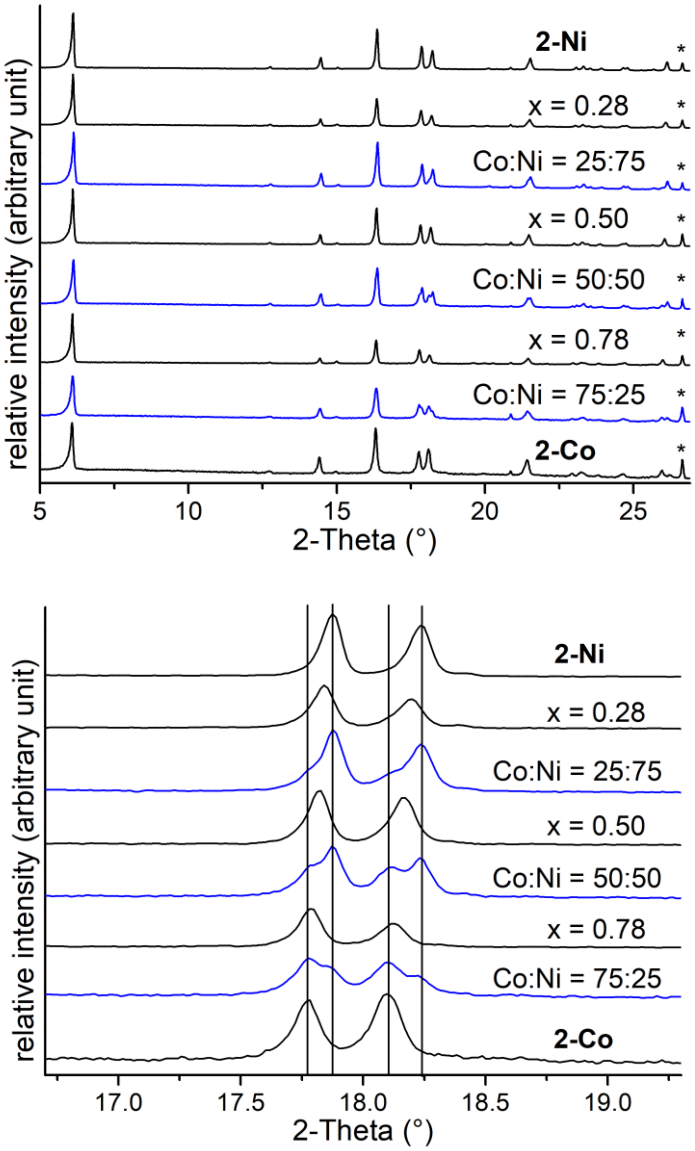

Figure S11. PXRD patterns for samples of mixed crystals of **2-Co$_x$Ni$_{1-x}$** (x = 0.28, 0.50, 0.78) synthesized at room temperature for 10 d in ethyl acetate together with the patterns of mixtures of **2-Co** and **2-Ni** with corresponding metal ratios in full (top) and larger range (bottom). The reflections indicated by an asterisk correspond to α-quartz as internal standard. The position of the -211 and -102 reflection for **2-Ni** and **2-Co** are indicated by solid lines.

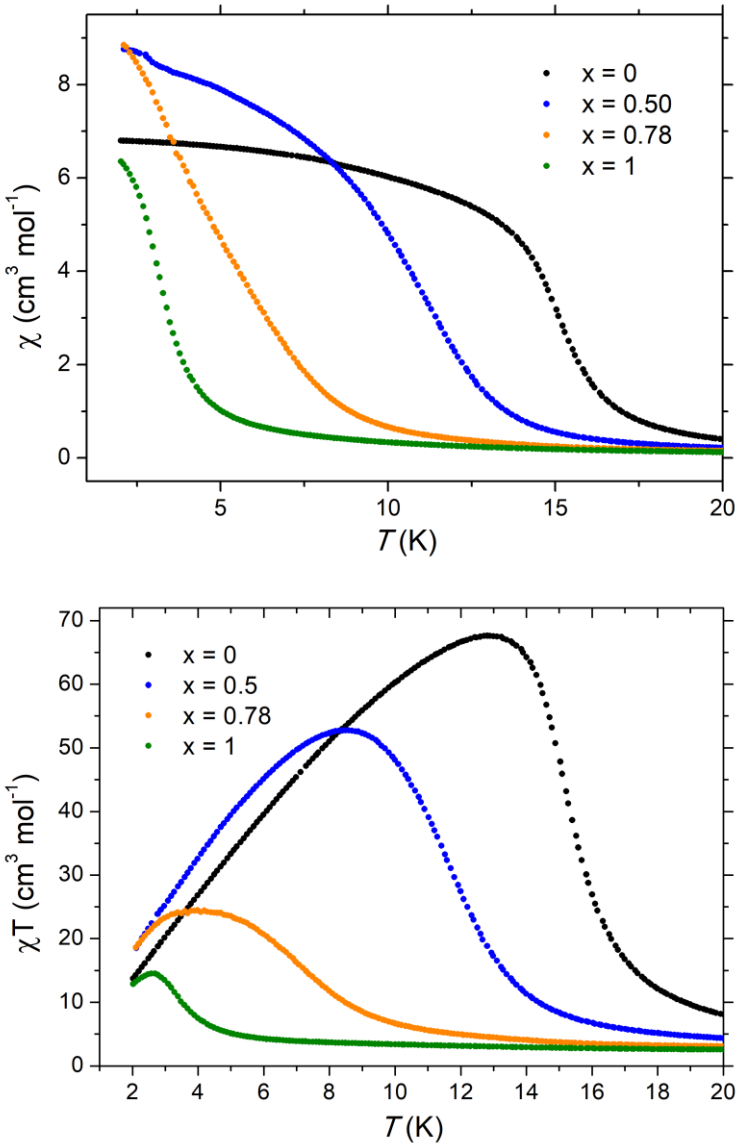

Figure S12. χ vs. T (top) and χT vs. T (bottom) measured in field of 1 kOe for samples of mixed crystals of **2-Co_xNi_{1-x}** (x = 0.50, 0.78) synthesized at room temperature for 10 d in ethyl acetate and for **2-Co** and **2-Ni**.

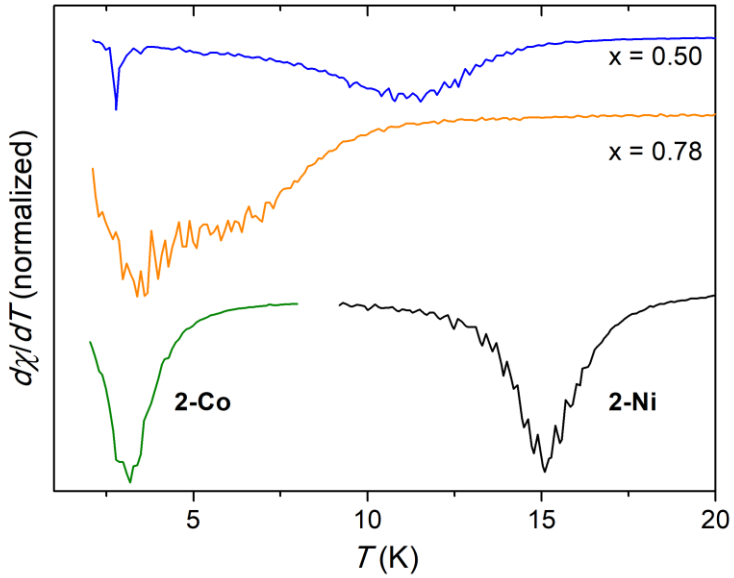

Figure S13. First derivative of the magnetic susceptibility for samples of mixed crystals of **2-Co_xNi_{1-x}** (x = 0.50, 0.78) synthesized at room temperature for 10 d in ethyl acetate and of **2-Co** and **2-Ni**.

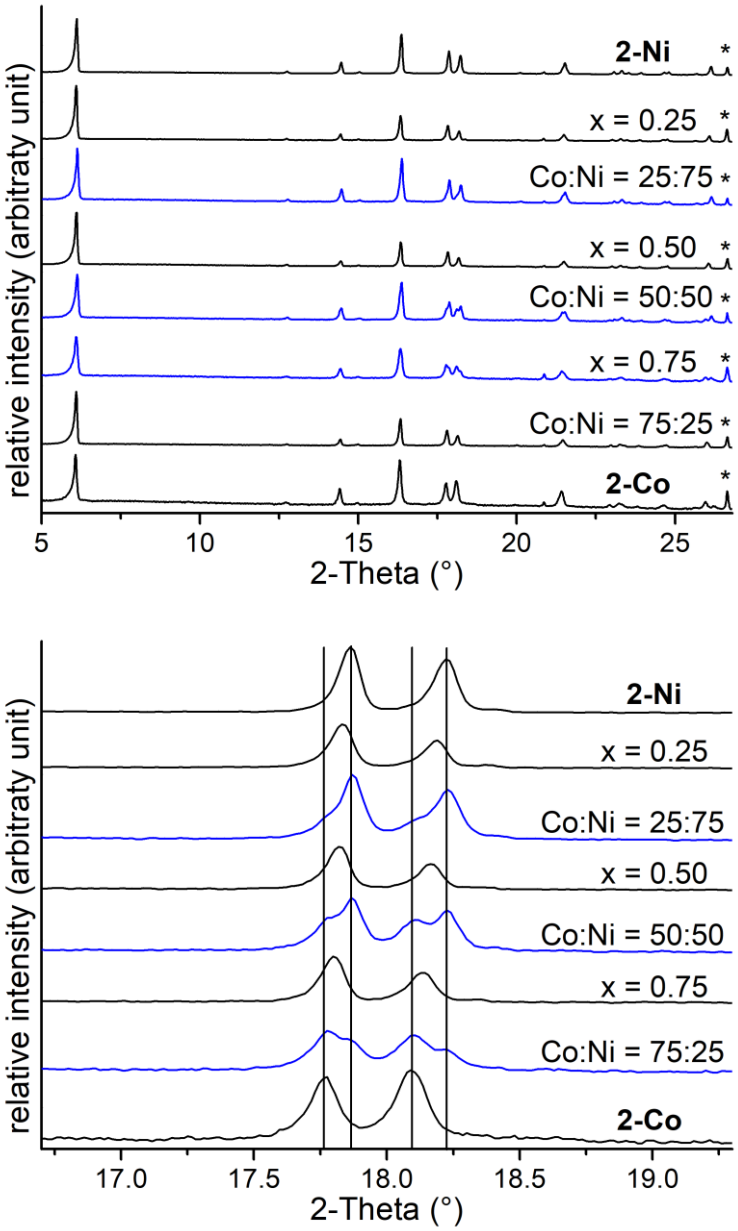

Figure S14. PXRD patterns for samples of mixed crystals of **2-Co$_x$Ni$_{1-x}$** (x = 0.25, 0.50, 0.75) synthesized at 70°C for 10 d together with the patterns of mixtures of **2-Co** and **2-Ni** with corresponding metal ratios in full range (top) and smaller range (bottom). The reaction mixture was filtrated after it was cooled to room temperature. In the top figure the reflections indicated by an asterisk correspond to α-quartz as internal standard. In the bottom figure the position of the reflection for **2-Ni** and **2-Co** are indicated by solid lines are the (-211) and (-102) reflections.

Table S2. Results of the AAS measurements for samples of mixed crystals of **2-Co_xNi_{1-x}** synthesized at 70°C for 10 d in ethyl acetate. The reaction mixture was filtrated after it was cooled to room temperature.

x **used in synthesis**	**0.25**	**0.60**	**0.80**
Sample 1	0.25	0.50	0.73
Sample 2	0.25	0.48	0.73
Sample 3	0.24	0.48	0.75
Average	**0.25**	**0.49**	**0.74**

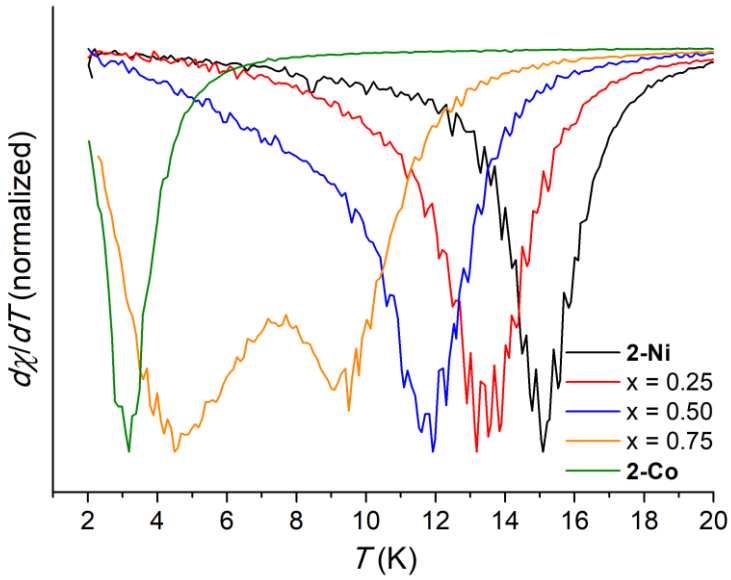

Figure S15. First derivative of the magnetization dχ/dT for samples of mixed crystals of **2-Co_xNi_{1-x}** (x = 0.25, 0.50, 0.75) synthesized at 70°C for 10 d in ethyl acetate together with the first derivative of **2-Co** and **2-Ni**. The reaction mixture was filtrated after it was cooled to room temperature.

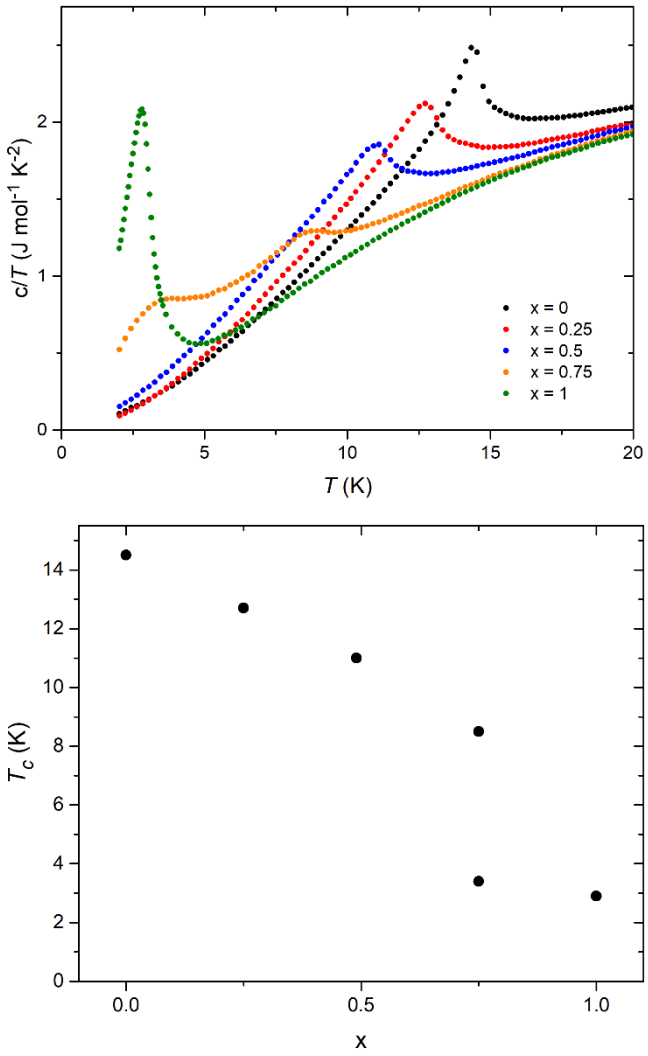

Figure S16. Temperature dependence of specific heat (top) and critical temperature determined from specific heat of mixed crystals **2-Co$_x$Ni$_{1-x}$** (x = 0.25, 0.50, 0.75) synthesized at 70°C for 10 d in ethyl acetate together with data for **2-Co** and **2-Ni**. For x = 0.75 two values are given, because two maxima are observed.

Table S3. Solubilities of $[M(NCS)_2(4\text{-tertbutylpyridine})]_n$, together with the solubilities of $[M(NCS)_2(4\text{-acetylpyridine})]_n$ and $[M(NCS)_2(\text{ethylisonicotinate})]_n$ (M=Co, Ni).

$[M(NCS)_2L_2]_n$	**M = Co**	**M = Ni**	**ratio**
Metal concentration	c(Co) [g/L]	c(Ni) [g/L]	
L= 4-tert-butylpyridine			
Sample 1	3.856	0.031	
Sample 2	3.786	0.028	
Sample 3	3.864	0.032	
average 1-3	3.835	0.030	
Solubility L = 4-tert-butylpyridine	29.0	0.231	125
Solubility L= 4-acetylpyridine	6.18	1.15	5.4
Solubility L= ethylisonicotinate	38.7	4.50	8.6

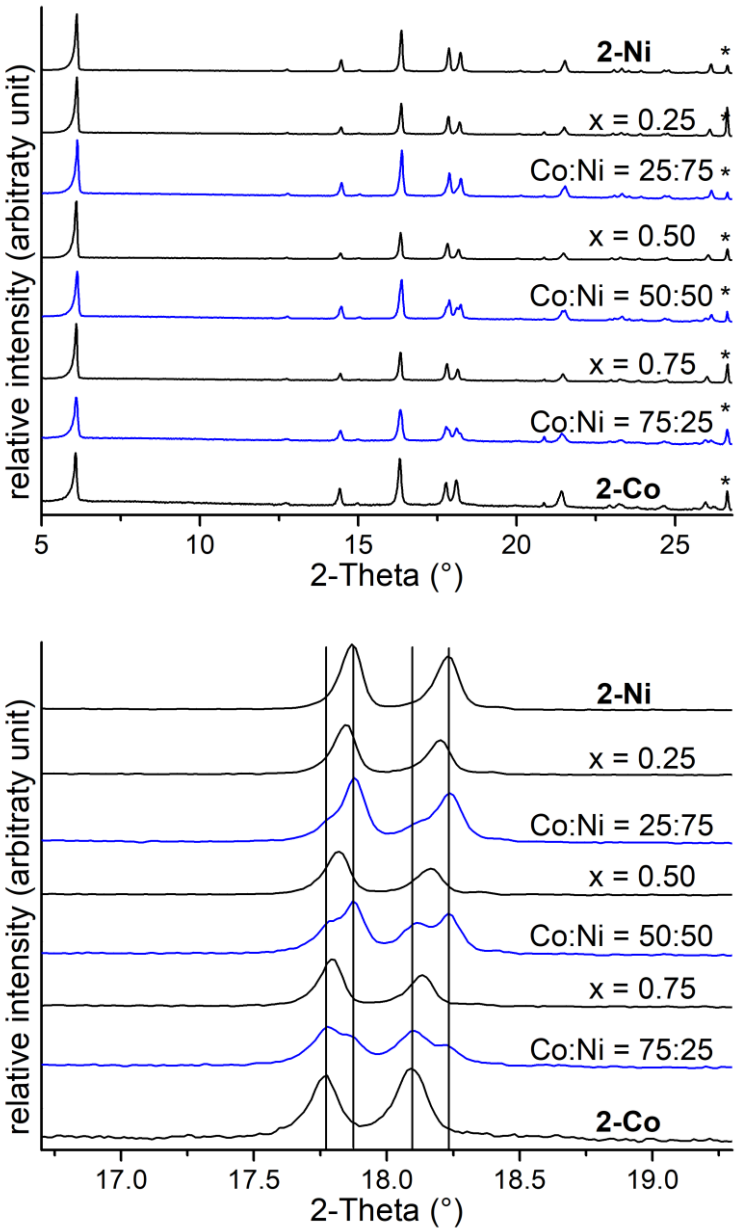

Figure S17. PXRD patterns for samples of mixed crystals of **2-Co$_x$Ni$_{1-x}$** (x = 0.25, 0.50, 0.75) synthesized at 70°C for 10 d in ethyl acetate, together with the patterns of mixtures of **2-Co** and **2-Ni** with corresponding metal ratios in full range (top) and smaller range (bottom). The reaction mixture was filtrated while still being at 70°C. In the top figure the reflections indicated by an asterisk correspond to α-quartz as internal standard. In the bottom figure the position of the reflection for **2-Ni** and **2-Co** are indicated by solid lines are the (-211) and (-102) reflections.

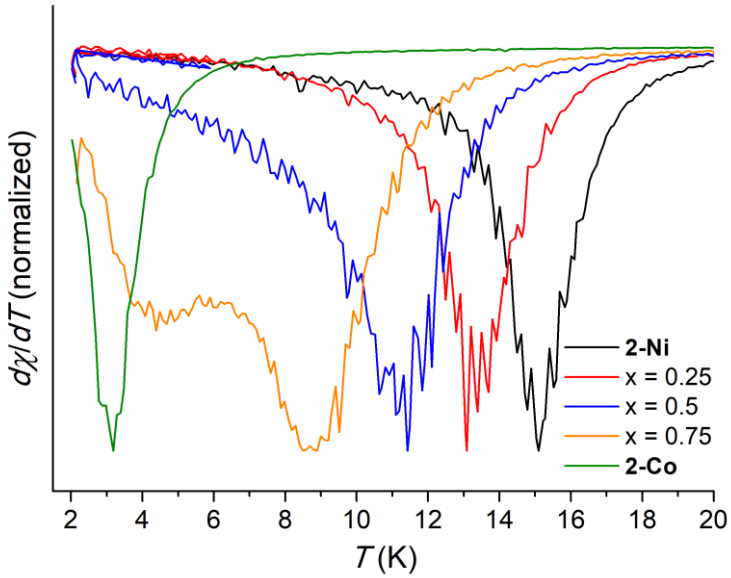

Figure S18. First derivative of the magnetization for samples of mixed crystals of **2-Co$_x$Ni$_{1-x}$** (x = 0.25, 0.50, 0.75) synthesized at 70°C for 10 d in ethyl acetate together with the first derivative of **2-Co** and **2-Ni**. The reaction mixture was filtrated while still being at 70°C.

Table S4. Results of the AAS measurements for samples of mixed crystals of **2-Co$_x$Ni$_{1-x}$** synthesized at 70°C for 10 d. The reaction mixture was filtrated while still being at 70°C.

***x* used in synthesis**	**0.25**	**0.60**	**0.80**
Sample 1	0.25	0.50	0.73
Sample 2	0.23	0.52	0.73
Sample 3	0.27	0.47	0.75
Average	**0.25**	**0.49**	**0.74**

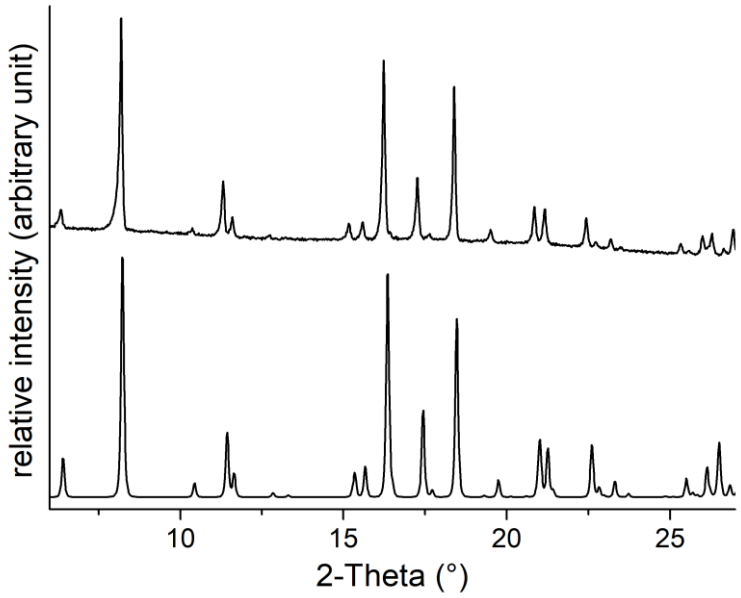

Figure S19. Experimental (top) and simulated powder pattern of **1**-**Co** (bottom).

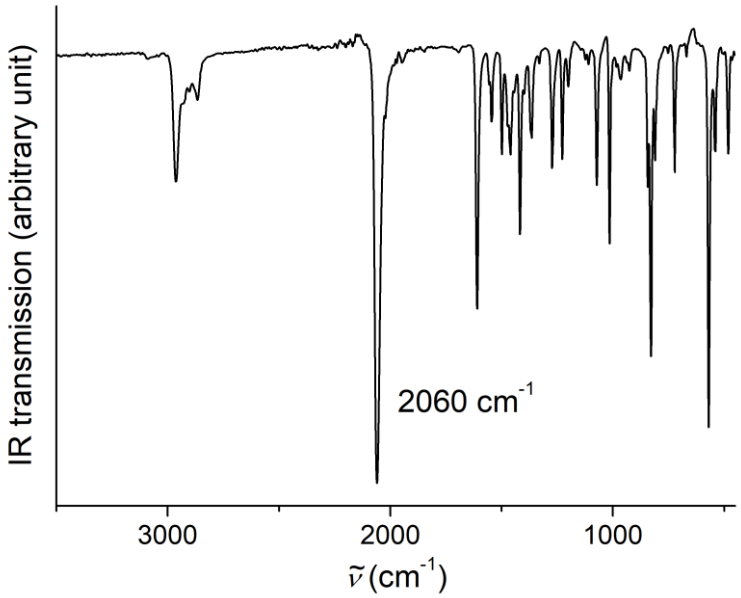

Figure S20. IR-spectrum of **1**-**Co**. Given is the value of the CN-stretching vibration.

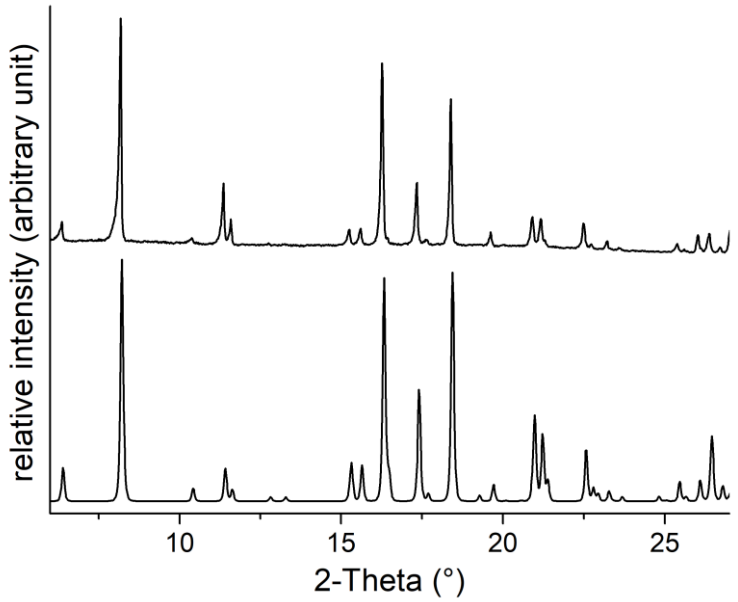

Figure S21. Experimental (top) and simulated powder pattern of **1**-Ni (bottom).

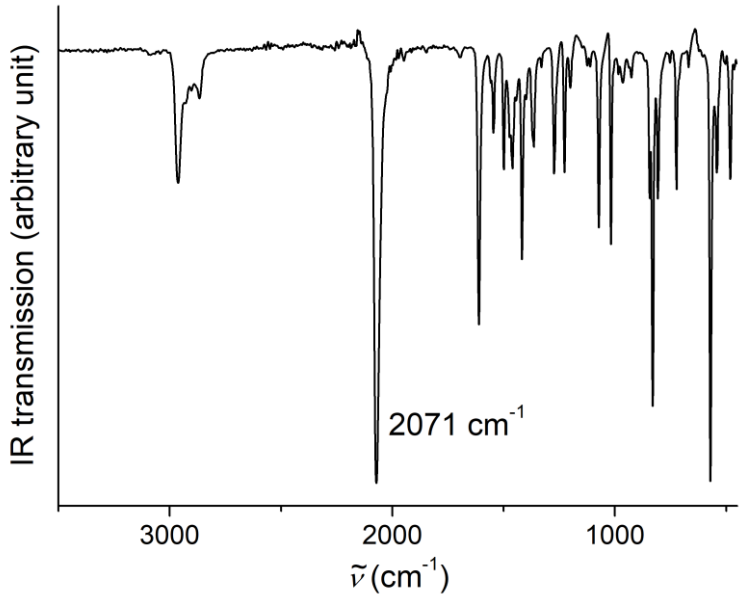

Figure S22. IR-spectrum of **1**-**Ni**. Given is the value of the CN-stretching vibration.

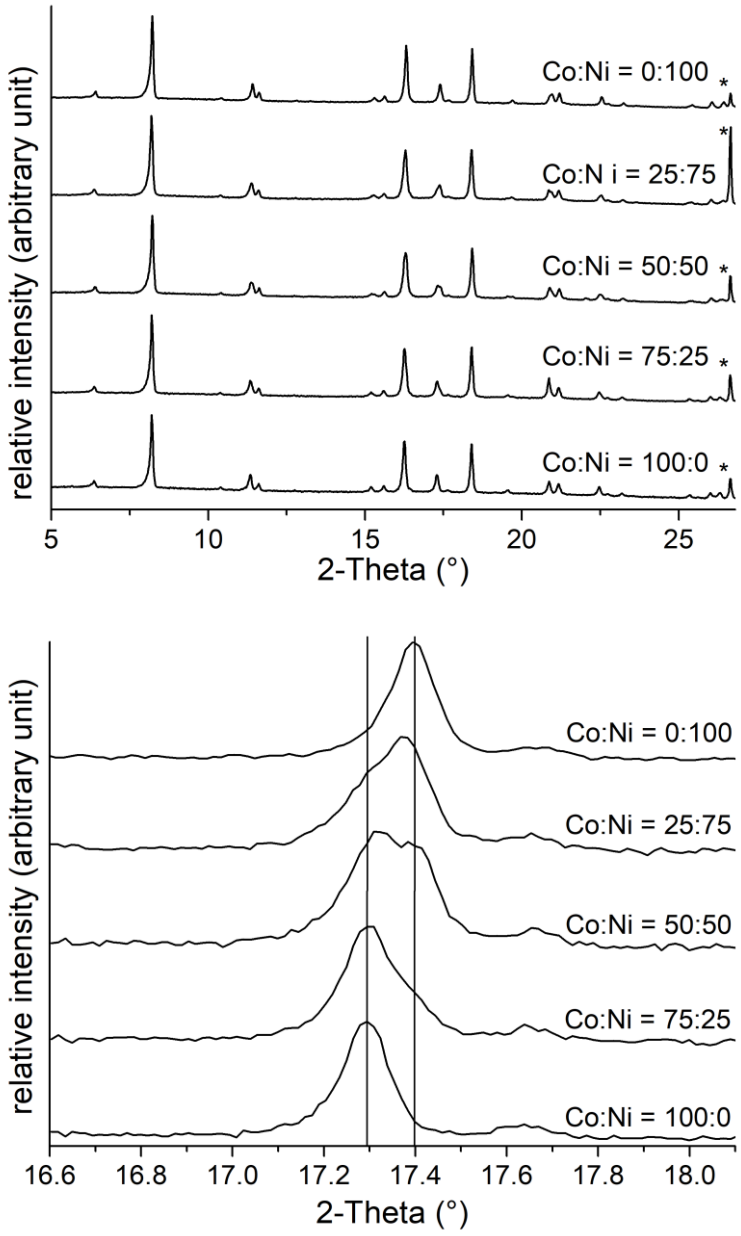

Figure S23. Experimental PXRD pattern of **1**-**Co**, **1**-**Ni** and of physical mixtures of **1-Co** and **1**-**Ni** in different Co:Ni ratios in full range (top) and smaller range (bottom). In the top figure the reflections indicated by an asterisk correspond to α-quartz as internal standard. In the bottom figure the position of the reflection for **1**-**Ni** and **1**-**Co** are indicated by solid lines are the (213) reflections.

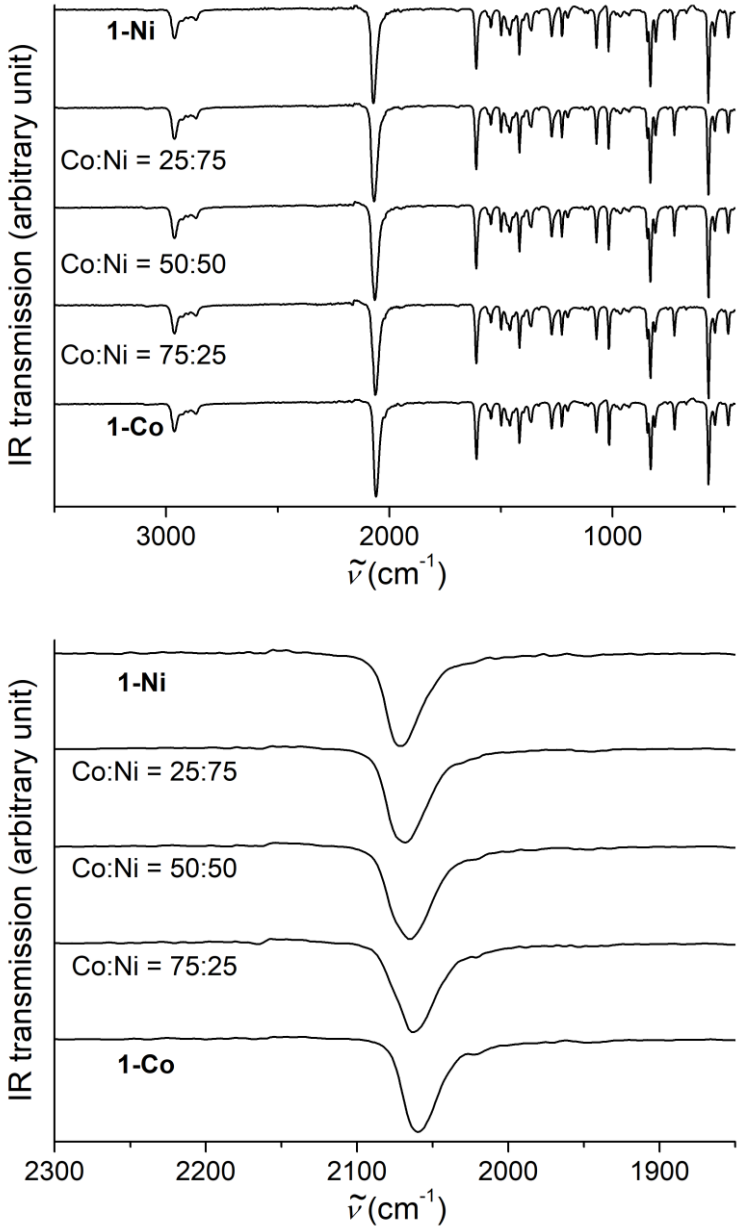

Figure S24. IR spectra of **1-Co**, **1-Ni** and of physical mixtures of **1**-**Co** and **1**-**Ni** in different Co:Ni ratios.

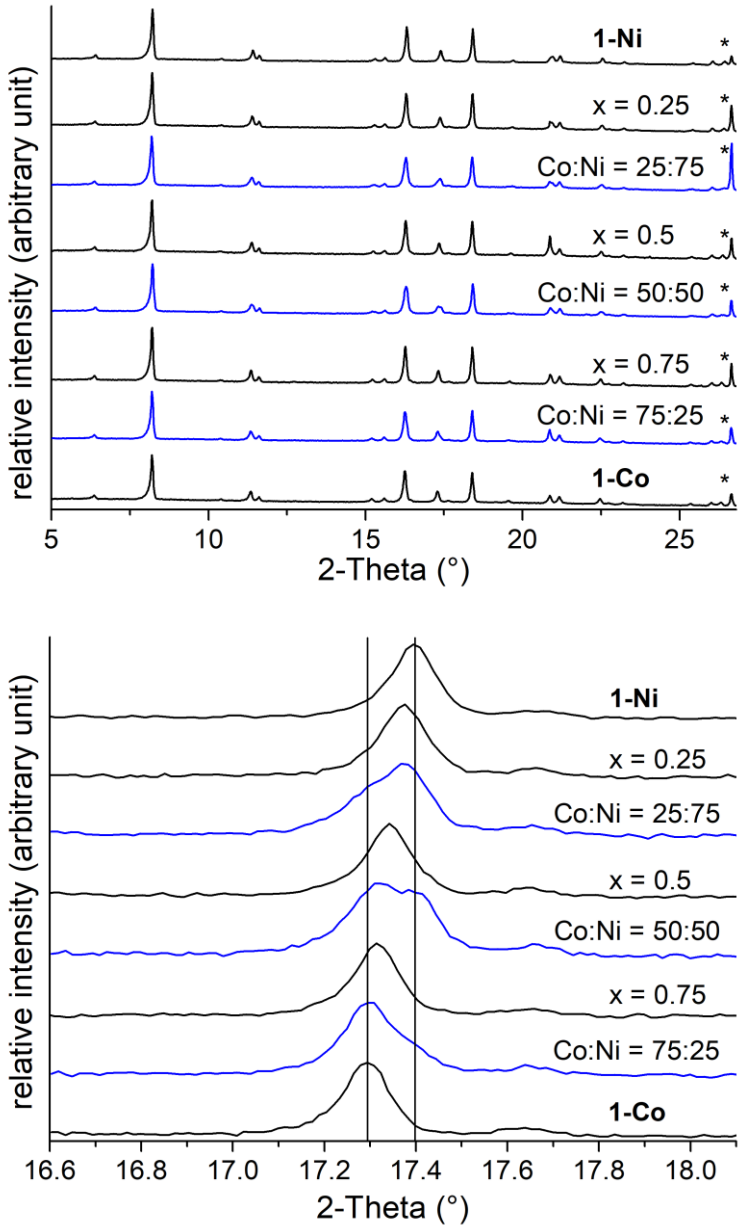

Figure S25. PXRD patterns for samples of mixed crystals of **1**-$\mathbf{Co_xNi_{1-x}}$ (x = 0.25, 0.50, 0.75), together with the patterns of mixtures of **1**-**Co** and **1**-**Ni** with corresponding metal ratios in full range (top) and a smaller range (bottom). In the top figure the reflections indicated by an asterisk correspond to α-quartz as internal standard. In the bottom figure the position of the reflection for **1**-**Ni** and **1**-**Co** are indicated by solid lines are the (213) reflections.

Table S5. Results of the AAS measurements for samples of mixed crystals of **1-Co_xNi_{1-x}**.

x **used in synthesis**	**0.25**	**0.5**	**0.75**
Sample 1	0.23	0.51	0.75
Sample 2	0.24	0.51	0.74
Sample 3	0.27	0.47	0.75
Average	**0.25**	**0.50**	**0.75**

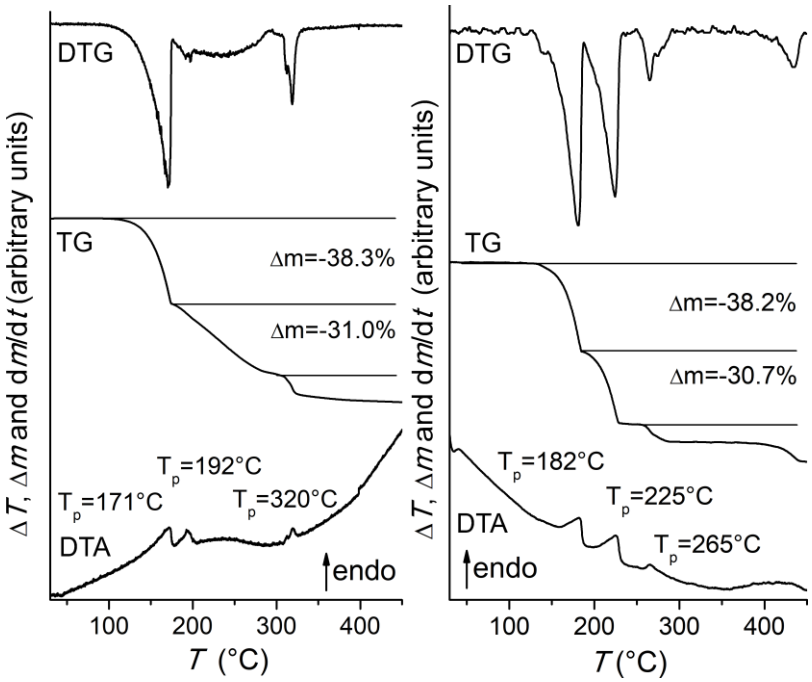

Figure S26. DTG, TG and DTA curves of **1-Co** (left) and **1-Ni** (right).

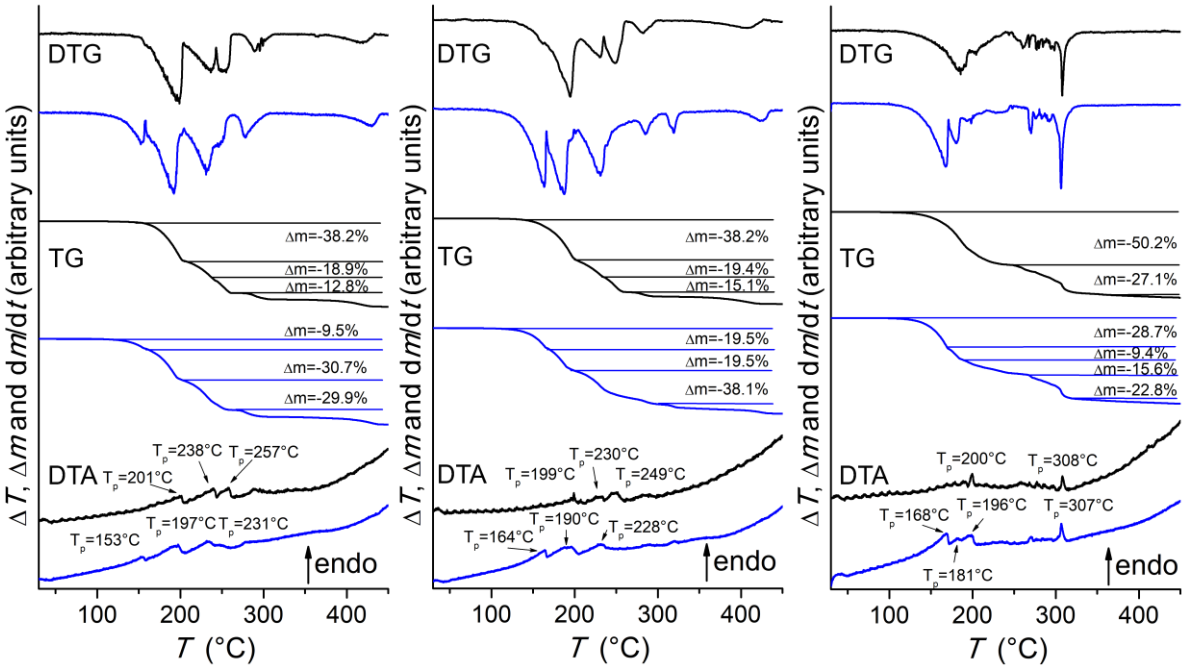

Figure S27. TG, DTG and DTA curves of **1**-$\mathbf{Co_xNi_{1-x}}$ for x = 0.25 (left), 0.50 (center) and 0.75 (right) (black) and of physical mixtures of **1-Co** and **1-Ni** with corresponding metal ratios (blue).

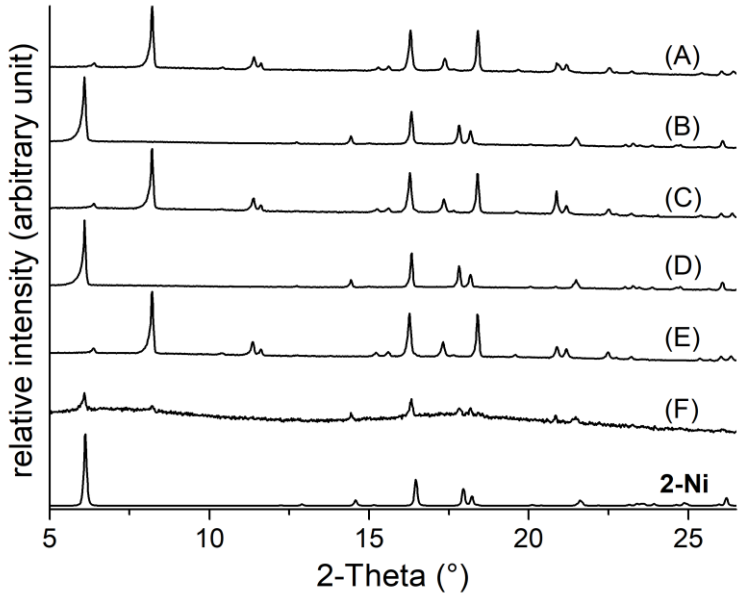

Figure S28. Experimental powder patterns of **1**-$\mathbf{Co_xNi_{1-x}}$ (x = 0.25 (A), 0.50 (C), 0.75 (E)) and of the residues obtained after a mass loss corresponding to the loss of two molecules 4-*tert*-butylpyridine (Δm = 37.8%) of **1**-$\mathbf{Co_xNi_{1-x}}$ (x = 0.25 (B), 0.50 (D), 0.75 (F)), together with the calculated powder pattern of **2-Ni**.

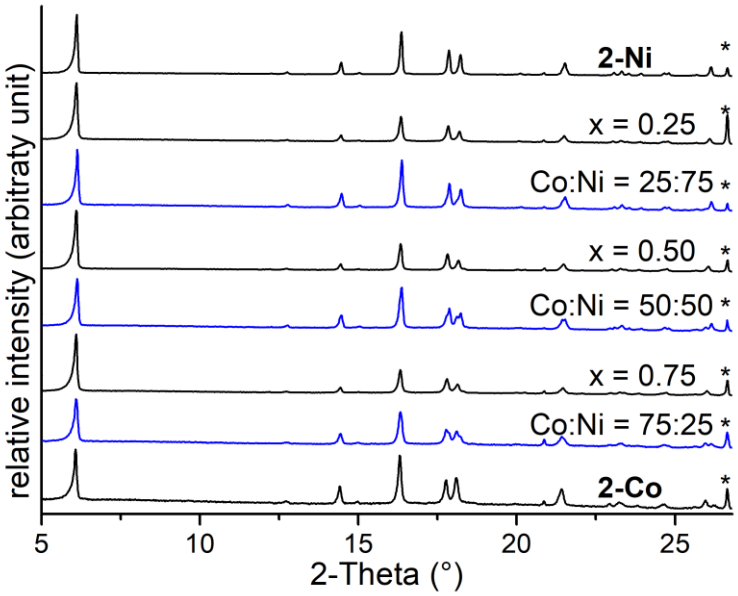

Figure S29. PXRD patterns for samples of mixed crystals of **2-Co$_x$Ni$_{1-x}$** (x = 0.25, 0.50, 0.75) synthesized at room temperature for 6 weeks in ethyl acetate, together with the patterns of mixtures of **2-Co** and **2-Ni** with corresponding metal ratios in full range (top) and smaller range (bottom). In the top figure the reflections indicated by an asterisk correspond to α-quartz as internal standard. In the bottom figure the position of the reflection for **2-Ni** and **2-Co** are indicated by solid lines are the (-211) and (-102) reflections.

Table S6. Results of the AAS measurements for samples of mixed crystals of **2-Co$_x$Ni$_{1-x}$** synthesized at room temperature with a reaction time of 6 weeks.

x **used in synthesis**	**0.3**	**0.55**	**0.8**
Sample 1	0.25	0.50	0.78
Sample 2	0.26	0.51	0.75
Sample 3	0.27	0.53	0.75
Average	**0.26**	**0.51**	**0.76**

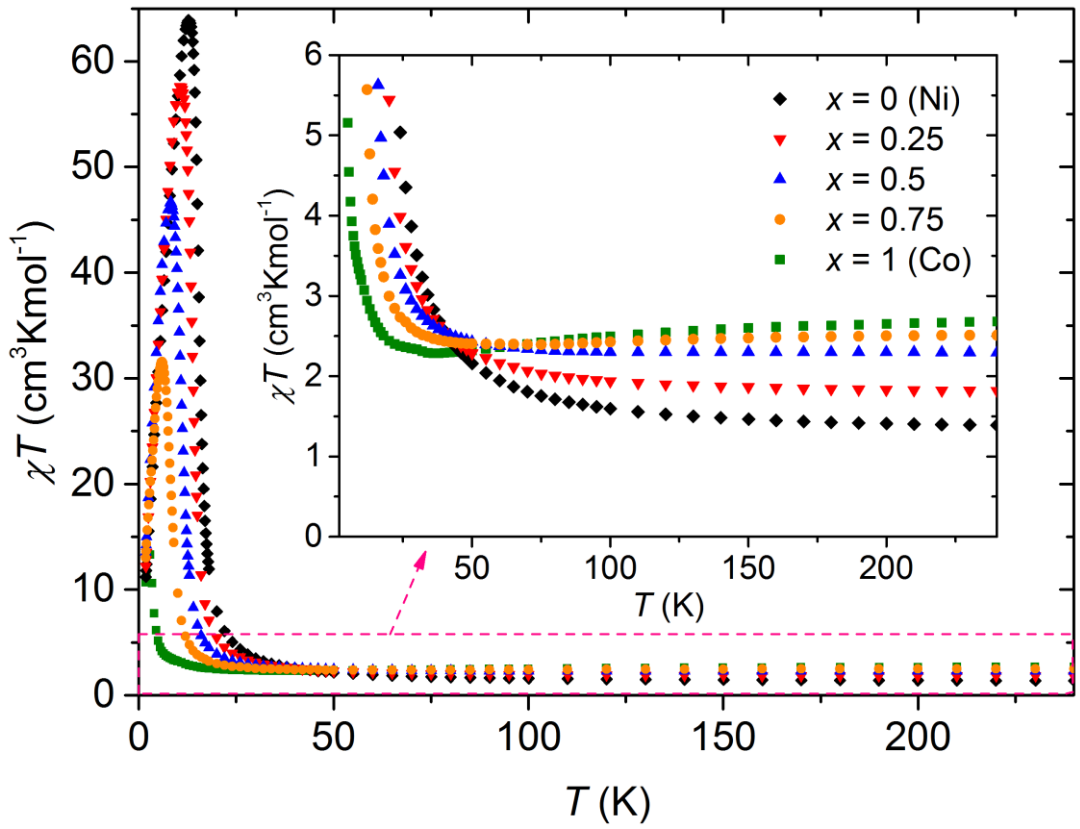

Figure S30. Magnetic susceptibility as a function of temperature measured in H = 1 kOe for **2-Co**, **2-Ni** and **2-Co_xNi_{1-x}** (x = 0.25, 0.5 and 0.75). Inset: magnification.

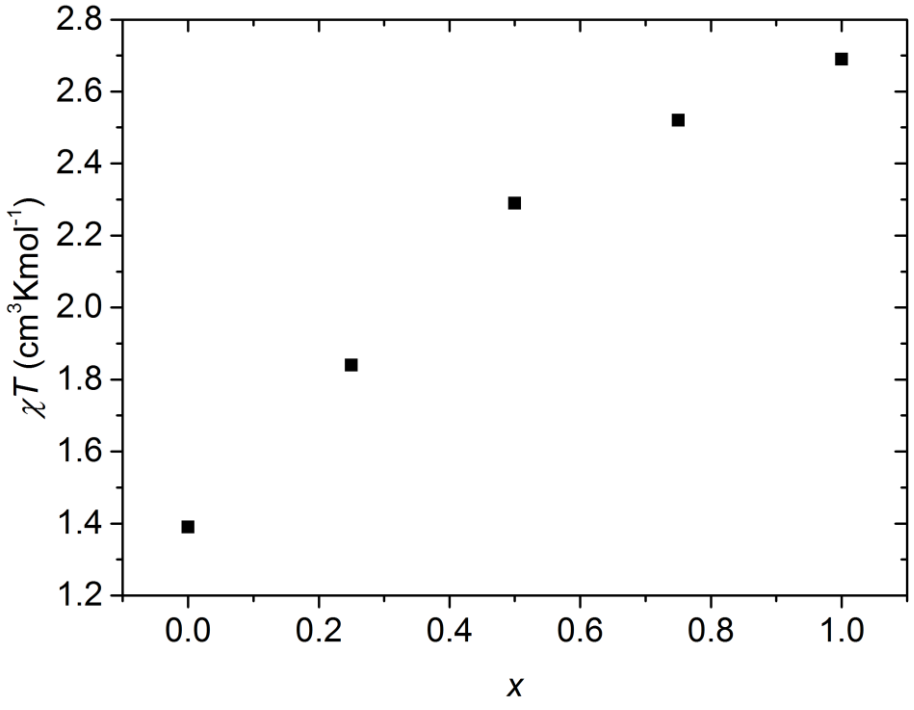

Figure S31. Magnetic susceptibility at 240 K measured in H = 1 kOe for **2-Co**, **2-Ni** and **2-Co_xNi_{1-x}** (x = 0.25, 0.5 and 0.75) as a function of x.

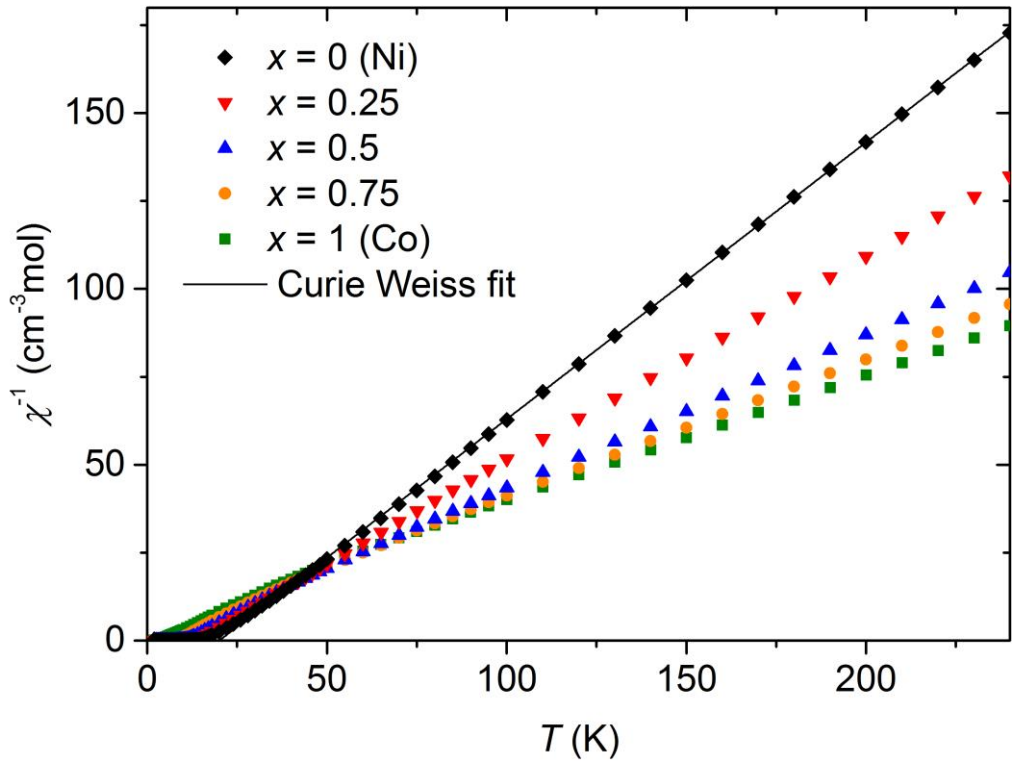

Figure S32. Inverse magnetic susceptibility versus temperature for of **2-Co**, **2-Ni** and **2-Co_xNi_{1-x}** (x = 0.25, 0.50 and 0.75). Solid line: Curie-Weiss fit to the data for **2-Ni**.

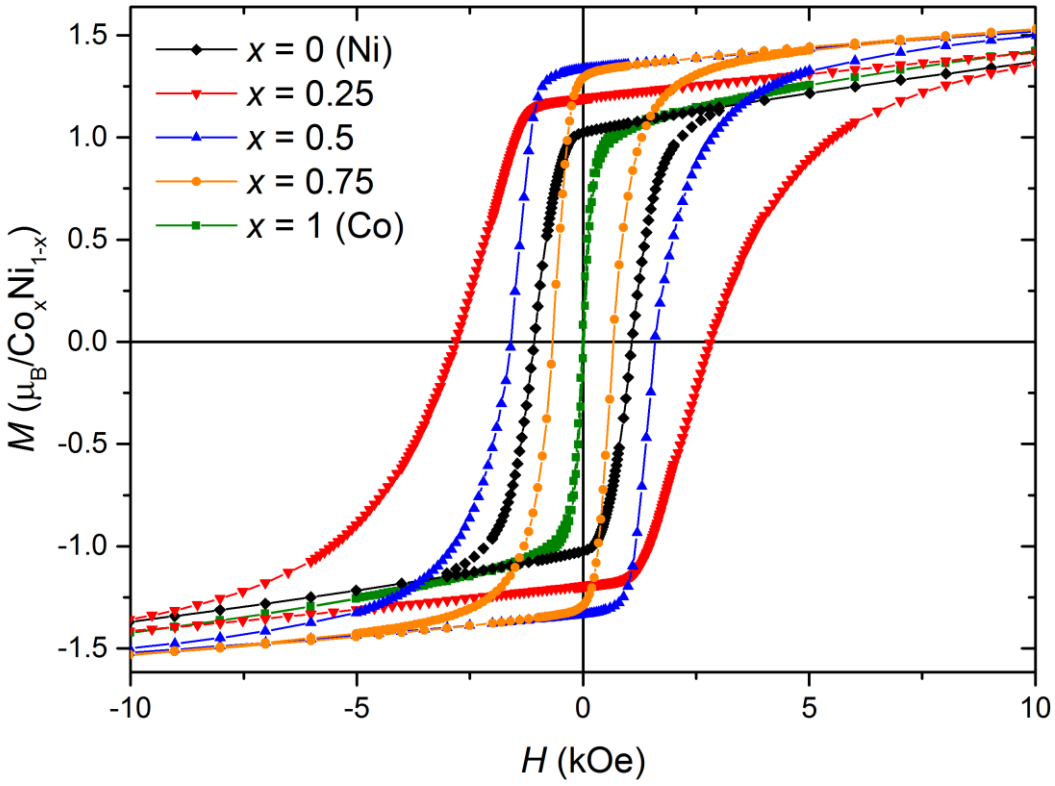

Figure S33. Magnetization vs. field measured at 1.8 K for **2-Co**, **2-Ni** and **2-Co_xNi_{1-x}** (x = 0.25, 0.5 and 0.75).

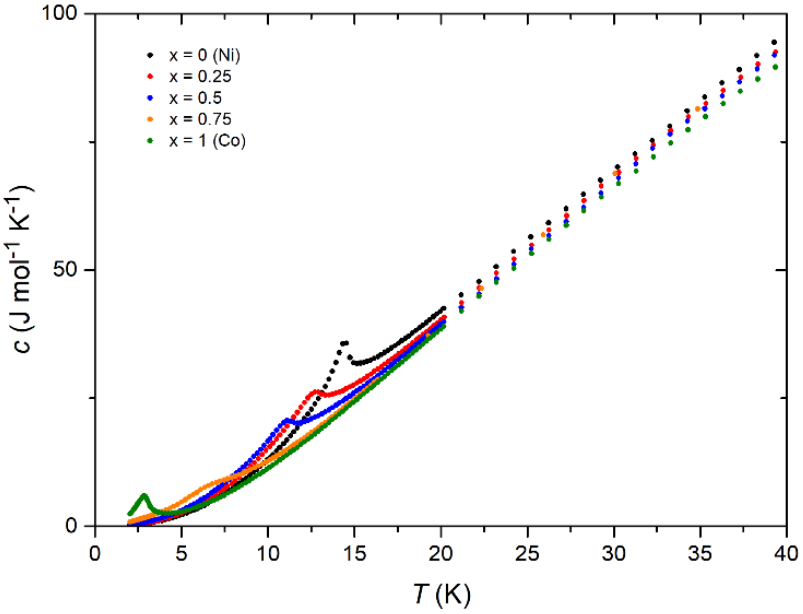

Figure S34. Specific heat of **2-Co**, **2-Ni** and **2-Co$_x$Ni$_{1-x}$**.

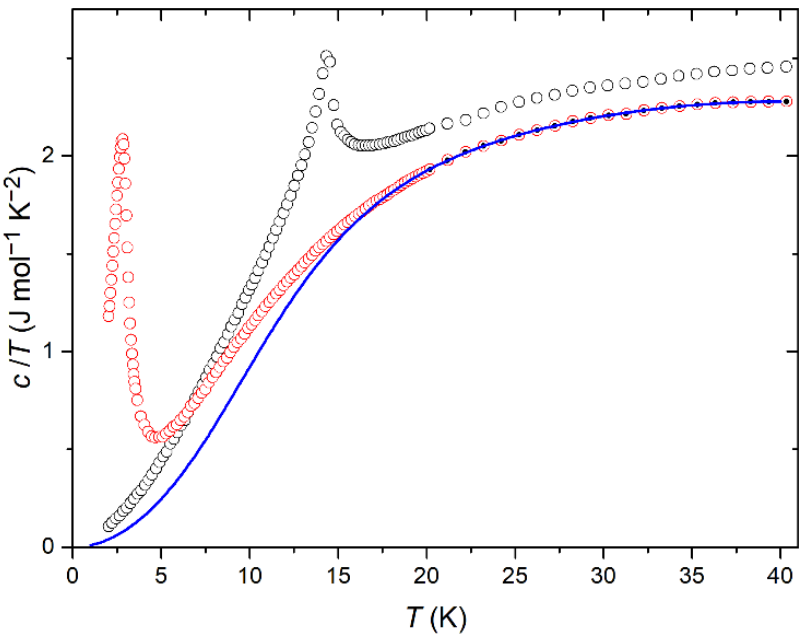

Figure S35. Estimation of the lattice specific heat. Data for **2-Co** (red points) in the range 20-40 K were used to fit a linear combination of Debye and Einstein models of lattice specific heat (solid line). Data for **2-Ni** (black points) are shown for comparison.

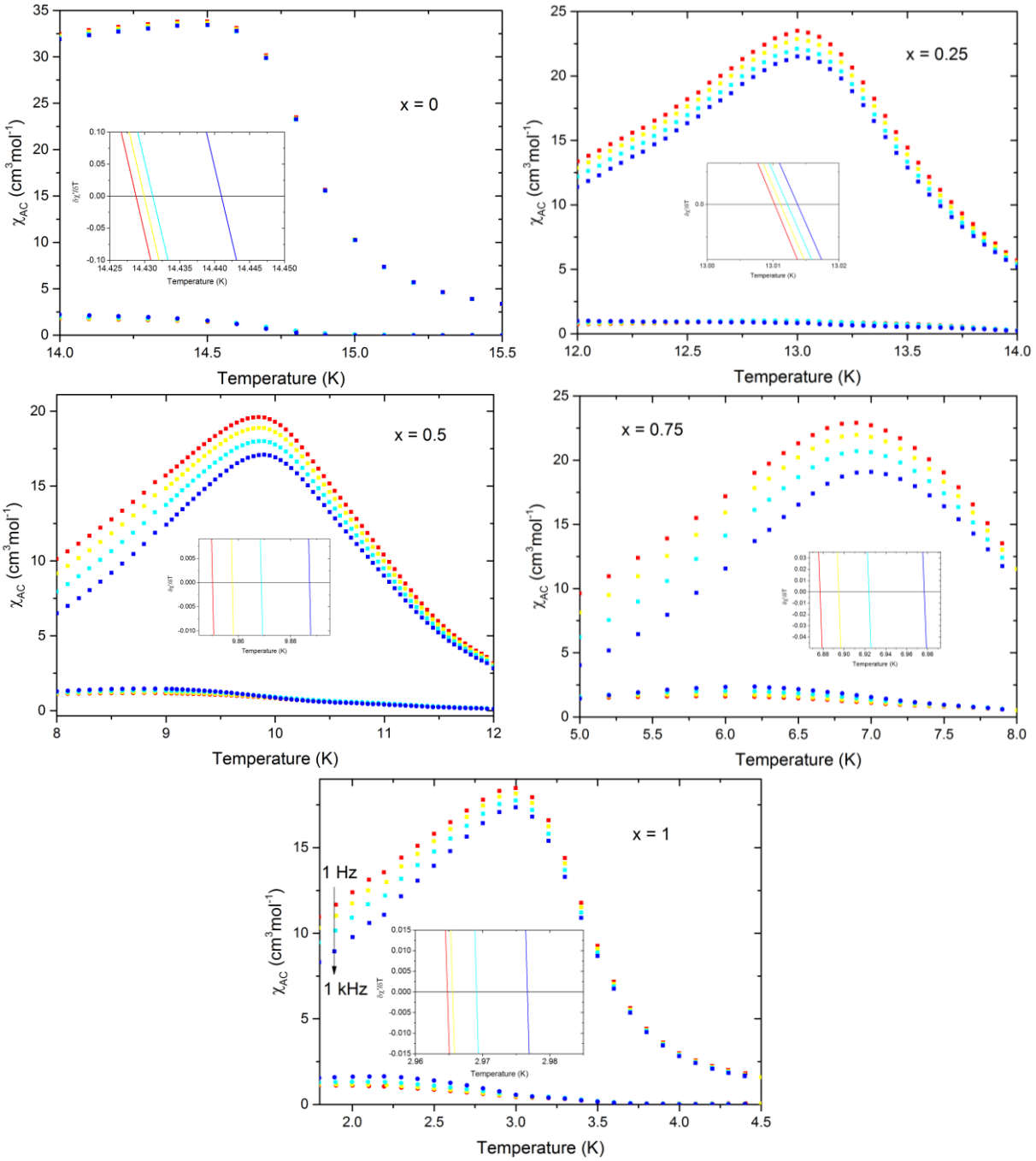

Figure S36. AC magnetic susceptibility vs. temperature for **2-Co**, **2-Ni** and **2-Co$_x$Ni$_{1-x}$** (x = 0.25, 0.50 and 0.75) synthesized at room-temperature for 6 weeks in ethyl acetate. Insets: derivative of χ' used to determine the peak positions.

Table S7. Mydosh parameter **2-Co**, **2-Ni** and **2-Co$_x$Ni$_{1-x}$** (x = 0.25, 0.50 and 0.75) synthesized at room-temperature for 6 weeks in ethyl acetate.

x	ϕ
1	0.00133(74)
0.75	0.0059(18)
0.50	0.00124(37)
0.25	0.000090(14)
0	0.00027(22)